

Discovery and Monitoring of a Broad Iron Line Complex in GRO J1655-40 by RXTE

Richard E. Rothschild*, William A. Heindl*, Jörn Wilms[†] and Rüdiger Staubert[†]

*CASS/UCSD, 0424, 9500 Gilman Dr., La Jolla, CA 92093

[†]IAA-A, Universität Tübingen, Sand 1, 72076 Tübingen, Germany

Abstract.

We present results from detailed spectral analyses of 43 RXTE observations of GRO J1655-40 made throughout 1996. Spectra taken over 27 days separated by about one week each allow us to determine 3-200 keV continuum and line variability during the thermally dominated and steep power-law states seen. Inferred effective radii for maximum disk emission are consistently below 6 gravitational radii, confirming the Kerr nature of the black hole. The broad iron line is modeled by a broad emission line and an absorption edge at ~ 6.7 keV. We discuss the variation in line and continuum parameters, and suggest the inner portion of the accretion disk is warped and hot.

INTRODUCTION

The black hole binary GRO J1655-40 was discovered on 1994 July 27 by the BASTE instrument on *CGRO* [1]. Radio observations made soon after the X-ray discovery of GRO J1655-40 revealed two superluminal components [2], thus classifying GRO J1655-40 as a microquasar. Analysis of a kinematic model for the bipolar jet emission yielded a jet velocity of $(0.92 \pm 0.02)c$, a jet inclination angle of $\sim 85^\circ$ and a distance of 3.2 ± 0.2 kpc [3]. The discovery of an optical counterpart [4] led to the determination of several system parameters, including a system inclination of $\sim 70^\circ$, and an orbital period of 2.62 days [5]. Modeling of optical light curves by several authors [6, 7, 8] all place the compact object mass in the 5–8 M_\odot range, establishing the black hole nature of the primary.

The black hole binary GRO J1655-40 experienced an extended outburst in 1996-1997 that was extensively observed by *RXTE* [9] and the 1996 luminosity is < 0.2 of the Eddington luminosity for a 6-7 M_\odot black hole. The X-ray spectral and temporal variability in the 1996-1997 outburst has been described in detail by Sobczak et al. [10] and Remillard et al. [11], respectively. They find four types of Quasi-Periodic Oscillations (QPOs) during 1996, three of which appear stable at 300 Hz, 9 Hz, and 0.1 Hz, and one which varies over the range 14–28 Hz.

The recent discovery of a second QPO frequency above 100 Hz [12] has strengthened the idea that the black hole is spinning, and possibly powering the jet emission. The innermost stable circular orbit (ISCO) radius for sub-Eddington accretion onto the black hole de-

pends upon the black hole angular momentum — the inner radius decreases from 6 GM/c^2 for a non-spinning Schwarzschild metric to 1.23 GM/c^2 for a maximally spinning Kerr metric. Emission lines from the inner parts of the accretion disk will experience Doppler and asymmetric relativistic broadening, and measurement of radii smaller than the Schwarzschild value can be taken as evidence for sub-Eddington luminosities from a spinning black hole. Iron line broadening has been reported recently for Galactic black hole binaries with two (XTE J1650-500 and XTE J1748-288) requiring the Kerr metric in the Very High state [13, 14]. Finally, Bałucińska-Church & Church [15] have reported the detection of red- and blue-shifted iron lines from the disk of GRO J1655-40 from one observation made on February 1997 by the Rossi X-ray Timing Explorer (*RXTE*) when the source was in the High/Soft state. Radii smaller than the Schwarzschild metric ISCO were *not* required for their analysis.

We present detailed spectral analysis of the 1996 data with an emphasis on line features present in the data.

BASIS FOR PCA SYSTEMATICS ESTIMATE

In order to perform detailed analysis of 5-10 keV spectral features at the few percent level, we first made an estimate of the PCA systematic error by fitting Crab observations over the period of time covered by the GRO J1655-40 observations. Ten short Crab observations and one long one were used. The long observation was used

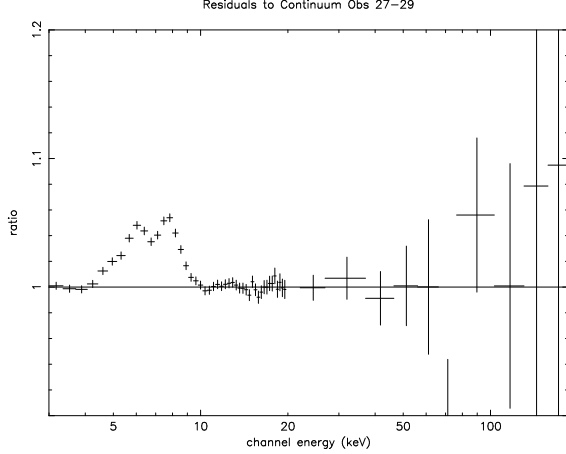


FIGURE 1. Residuals to the continuum fit omitting ~ 5 -10 keV in the fitting expressed as the ratio of the data to the model. See the text for a description of the modeling.

to estimate the systematics inherent in a single observation and the short observations were used to estimate the longer term systematic effects due to gain variations and systematics in background estimation spread over 17 months. All 3-20 keV PCA spectra were fitted to two absorbed power laws — the pulsar power law was held at a photon index of 1.63 [16] and 10% flux relative to the nebular flux, while the line of sight absorption, nebular index, and nebular flux were free to vary. We determined that ~ 0.1 – 0.2% systematics was sufficient for all but four energy channels. The lowest channel (#4) required 1% as did #10. Channels 9 and 11 were set to 0.5%. These systematics allow a fit to the Crab with $\chi^2_V = 0.55$ for the long and 1.50 for simultaneously fitting the eight short observations. This procedure resulted in $\Gamma_N = 2.20 \pm 0.01$ and $N_H = 0.86 \pm 0.04$. We feel that this set of systematic values are appropriate for the present analysis, and no additional systematic errors were incorporated in the HEXTE data, because the statistical errors were larger than the few percent systematic errors reported in Rothschild et al. [17].

SPECTRAL CONTINUUM FITTING

We initially modeled the spectra with low energy absorption (XSPEC model: `phabs`), free to vary, modifying the sum of a multicolored disk (`diskbb`), and a broken power law (`bknpower`), using XSPEC 11.2 [18]. A break in the power law was required for some of the observations, and the break energy was set to 300 keV for those observations with no apparent break. An F-test probability less than 1×10^{-3} was required for a break to be used. The broken power law and HEXTE data were used for Observations 25 to 47, where significant flux above 20 keV was detected. Observations 5-29, before

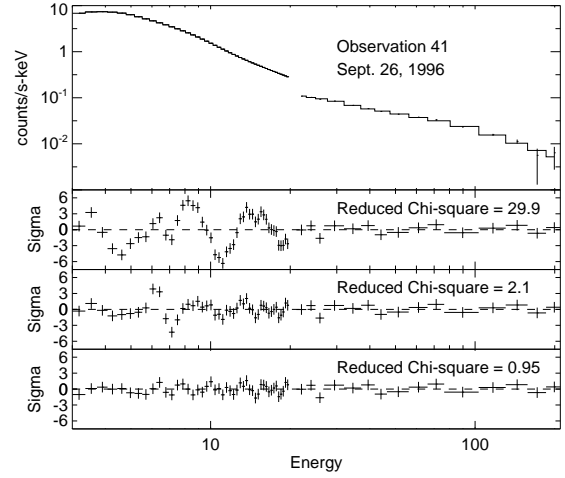


FIGURE 2. Residuals to the continuum fit omitting ~ 5 -10 keV in the fitting expressed in units of standard deviations (i.e., delchi). Residuals: (top) continuum only, (middle) continuum plus gauss, (bottom) continuum plus gauss plus edge.

the flat power law component appeared, required the addition of a broad soft component that we modeled as a blackbody. Models using a steep power law instead of the blackbody provided worse fits. In all observations significant deviations from the model existed in the 5-10 keV band. We then ignored PCA data from ~ 5 to ~ 10 keV and fit the continuum model again with the result that reduced chi-square was on the order of 1. Figure 1 shows a typical residual to the continuum fit when the 5-10 keV PCA data are again present but no subsequent fitting has been performed.

SPECTRAL LINE FITTING

Starting with the continuum fit parameters from when the 5-10 keV band was ignored, we first fit the entire 3-200 keV spectrum with just the continuum model. To this we added a gaussian line (`gauss`) and found the best fit with centroid, width and flux free to vary. The χ^2 was still unacceptably high. To this model, we added an absorption edge (`edge`) modifying the entire continuum model, again with edge energy and optical depth free. This yielded an acceptable χ^2 . Using Observation 41, which occurred on 1996, Sept. 26, as an example, we show the effects of sequentially adding the line and edge in Fig. 2. This model worked in general, and is the basis for our interpretation of the GRO J1655-40 system.

DISCUSSION

Emission States

Utilizing the characterization of black hole emission states of McClintock & Remillard [19], GRO J1655-40 began in the thermal dominated (TD) state before the power law component appeared, and then oscillated between the TD and steep power-law (SPL) states throughout most of 1996. The SPL states were accompanied by QPO detections while the TD states were not [9]. Transitions from one state to another occurred from one observation to another or over two or three observations. In contrast to the previous nomenclature of very high (VH) or high/soft (HS) states, where GRO J1655-40 was described as being in the VH state in 1996, the source changes state much more often in this characterization. On 5 of the 27 days, GRO J1655-40 had power law flux greater than 50% of the total flux, and on 11 of 27 days, it had greater than 20% of the total flux.

Inferred Inner Radii and Black Hole Spin

The value of the inferred inner radius of the accretion disk can be used to separate spinning (i.e., Kerr metric) from non-spinning (Schwarzschild metric) black holes. The innermost stable circular orbit (ISCO) for non-spinning black holes is $6 R_g$, and is $1.235 R_g$ for a maximally spinning (maximal Kerr metric) black hole, where $R_g = GM/c^2$. Thus, one would have strong evidence for a spinning black hole if one inferred an effective radius between these values.

We made cuts on the data for observations in which the multicolor disk component dominated the total 2-10 keV emission (i.e., the TD state where disk flux is greater than half of the total flux). Using the formulation of Merloni, Fabian, & Ross [20] ($R_{eff} = \eta g(i) f^2 R_{col}$ and $kT_{eff} = kT_{col}/f$), we can compute the effective radii in terms of gravitational radii with $\eta g(i) = 0.5$, the spectral hardening $f = 1.7$, $M = 7 M_\odot$ [7], $D = 3.2$ kpc [3], and $i = 69^\circ$ [6]. For TD state observations in 1996, the inferred effective radius R_{eff} begins at the ISCO for a maximally spinning black hole and moves out to $R_{eff} \approx 3R_g$ once the power law component is established.

When we include the radii inferred from the blackbody component present in the first seven observations, the blackbody radii values also cluster at the Kerr minimum value, and to some extent add to the inference that the disk extends inward beyond the Schwarzschild value of $6 R_g$. We note that Shrader & Titarchuk [21] have pointed out, however, that if the bulk flow model is correct, then emission from the inner radii of the accretion disk is unobservable. In this case, inferences about the in-

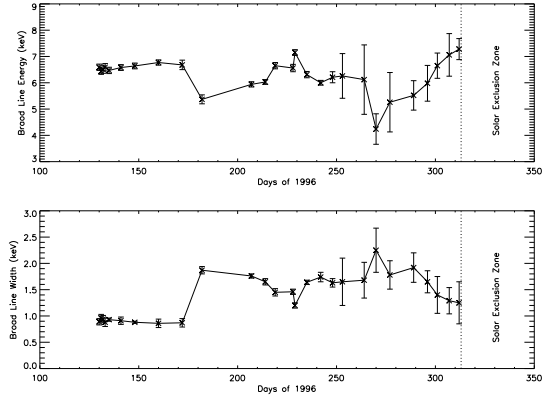


FIGURE 3. The edge energy (Top) and the optical depth (Bottom) for observations made in 1996 of GRO J1655-40.

ner radius cannot be made.

Absorption Edge and Accretion Disk Warp

Initially, before the appearance of the power law component, the edge energy was ~ 6.4 keV with an optical depth of ~ 0.2 (see fig. 3). The establishment of the power law was coincident with an increase in the energy of the edge to ~ 6.8 keV and a drop in the optical depth to ~ 0.04 . We investigated if a correlation existed between the absorbing column, N_H and the optical depth, which might suggest the absorbing column was responsible for the edge. No such correlation was found. Indeed, both the high and lower levels of the optical depth were present along with a wide range of values of the absorbing column.

As mentioned in the Introduction, the inclination angle of the radio jet was significantly higher than that of the orbital plane ($\sim 85^\circ$ versus 70°) and was near edge-on. The presence of the absorption edge can be understood if we are viewing the inner disk emission through portions of the disk. The edge energy implies highly ionized iron, and therefore the intervening material must also be part of the inner accretion disk (or heated by some other mechanism). This can be accomplished by a warp in the inner portions of the disk. When considered along with a requirement for the outer portions to be warped also [22], we conclude that a warped disk is present.

The models also agree on the large inclination angle ($\sim 70^\circ$) for the orbital plane, in contrast to the jet inclination angle. Assuming the jet to be perpendicular to the inner accretion disk plane, this portion of the disk is not in the orbital plane, again suggesting a warped accretion disk is present at GRO J1655-40. Indeed, Esin, Lasota, & Hynes [22] require the outer portions of the GRO J1655-

40 accretion disk to be warped during outburst to reconcile the X-ray and optical data.

The change in edge energy from ~ 6.4 keV to ~ 6.8 keV in coincidence with the appearance of the power law is further evidence of a hot corona being the source of the power law through Compton up-scattering. The same inner disk material that produced the “cool” edge initially, became significantly “hotter” later. The duration of the cooler material (~ 45 days) may be indicative of the timescale to heat the corona.

Broad Line Variability

As can be seen in Fig. 4, the centroid energy of the broad emission line varied about ~ 6.5 keV throughout 1996 with some deviations above and below that value. While the width of the line was initially ~ 1.0 keV, it jumped to ~ 1.7 keV with the appearance of the power law. Once at 1.7 keV, the width appears to be anti-correlated to the centroid energy. When the energy goes down, the width goes up and visa-versa. The broad line flux varies from 0.1 to 0.6 photons/cm²-s with no obvious correlation with other parameters. Finally, the equivalent width shows a slow decline from 600 eV to 200 eV over the observations in 1996, with the exception of a jump to 1200 eV just before the appearance of the power law.

Reynolds & Nowak [23] have modeled the expected iron line profiles from relativistic accretion disks as a function of disk inclination. For inclinations near edge-on, as is the case for GRO J1655-40, the line broadens and does not show the “more traditional” profile described by the *Laor* function. In addition, Armitage & Nowak [24] simulations of accretion structure that might be observed from an edge-on disk (their Fig.4 (lower right)) reveal a complex emission region. Consequently, we expect the total iron line complex to be very complicated, and a broad line approximation is acceptable, especially considering the limited energy resolution (but excellent statistics) of the PCA.

REFERENCES

1. Zhang, S.N. et al. 1994, IAU Circ. 6046.
2. Tingay, S.J. et al. 1995, Nature, 374, 141.
3. Hjellming, R.M. & Rupen, M.P. 1995, Nature, 375, 464.
4. Bailyn, C.D. et al. 1995, Nature, 374, 701.
5. Orosz, J.A. & Bailyn, C.D. 1997, Ap.J., 477, 876.
6. van der Hooft, F. et al. 1997, M.N.R.A.S., 286, L43.
7. Shahbaz, T., van der Hooft, F., Casares, J., Charles, P.A., & van Paradijs, J. 1999, M.N.R.A.S., 306, 89.
8. Green, J., Bailyn, & Orosz 2001, Ap.J., 554, 1290.
9. Remillard, R.A., Bradt, H., Cui, W., Levine, A.M., Morgan, E.H., Shirey, B. & Smith, D. 1996, IAU Circ. 6393.

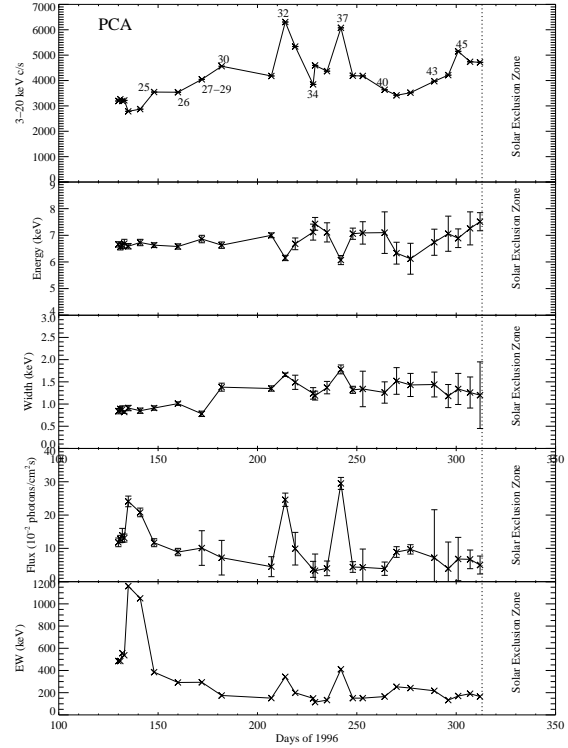


FIGURE 4. From Top to Bottom: The PCA count rate, broad line centroid energy, width, flux, and equivalent width for observations made in 1996 of GRO J1655-40.

10. Sobczak, G.J., McClintock, J.E., Remillard, R.A., Bailyn, C.D., & Orosz, J.A. 1999, Ap.J, 520, 776.
11. Remillard, R.A., Morgan, E.H., McClintock, J.E., Bailyn, C.D., & Orosz, J.A. 1999, Ap.J, 522, 397.
12. Strohmayer, T.E. 2001, Ap.J, 552, L49.
13. Miller, J.M. et al. 2001, Ap.J, 546, 1055.
14. Miller, J.M. et al. 2002b, Ap.J, 570, L69.
15. Bałucińska-Church, M. & Church, M.J. 2000, M.N.R.A.S., 312, L55.
16. Willingale, R. et al. 2001 A&A, 365, L212.
17. Rothschild, R.E. et al. 1998, Ap.J., 496, 538.
18. Arnaud, K.A. 1996, Astronomical Data Analysis Software and Systems V, eds. Jacoby, G. & Barnes, J., ASP Conf. Series 101, 17.
19. McClintock, J.E. & Remillard, R.A. 2003 astro-ph/0306213_v2.
20. Merloni, A., Fabian, A.C., & Ross, R.R. 2000, M.N.R.A.S., 313, 193.
21. Shrader, C.R. & Titarchuk, L. 2003, Ap.J., 598, 168.
22. Esin, A.A., Lasota, J.-P., & Hynes, R.I. 2000, A&A, 354, 987.
23. Reynolds, C.S. & Nowak, M.A. 2003, Phys. Rept., 377, 389.
24. Armitage, P.J. & Nowak, M.A. 2003, M.N.R.A.S., 341, 1041.